AlN photonic crystal nanocavities realized by epitaxial conformal growth on nanopatterned silicon substrate

D. Néel,[1,a)] S. Sergent,[2,3] M. Mexis,[4] D. Sam-Giao,[5] T. Guillet,[4] C. Brimont,[4] T. Bretagnon,[4] F. Semond,[2] B. Gayral,[5] S. David,[1] X. Checoury,[1] and P. Boucaud[1]

[1]*Institut d'Électronique Fondamentale, UMR CNRS 8622, Université Paris Sud-11, F-91405 Orsay, France*
[2]*CRHEA-CNRS, Rue Bernard Grégory, 06560 Valbonne, France*
[3]*Université de Nice Sophia Antipolis, Parc Valrose, F-06102 Nice Cedex 2, France*
[4]*Université Montpellier 2, Laboratoire Charles Coulomb, CNRS UMR 5221, F-34095 Montpellier, France*
[5]*CEA-CNRS group "Nanophysique et semiconducteurs," INAC-SP2M, CEA-Grenoble, 17 rue des Martyrs, 38054 Grenoble Cedex 9, France*

An original method to fabricate III-nitride photonic crystal membranes without etching of III-N materials is reported. A photonic crystal pattern is first realized in a silicon substrate. GaN quantum dots embedded in a thin AlN layer are then grown by conformal epitaxy using ammonia-based molecular beam epitaxy on the top of the patterned silicon substrate and a free-standing membrane is achieved by selective etching of the silicon substrate through the holes of the photonic crystal. Room temperature microphotoluminescence measurements show a quality factor as high as 1800 at 425 nm on a modified $L3$ cavity. Possibility to achieve lasing with this system is discussed. © *2011 American Institute of Physics*. [doi:10.1063/1.3605592]

III-N materials (GaN, AlN, InN, and related alloys) have become the dominant materials for UV to blue-green semiconductor light sources. The success in the development of these materials has allowed to market blue, green, and white light-emitting diodes but also blue lasers. It is recognized that the achievement of compact III-N lasers integrated with the silicon technology would represent a significant advance for future developments. In parallel, recent works on photonic crystal resonators have demonstrated the potential of these structures to achieve optical modes with high quality factor (Q) values within small modal volumes, allowing the observation of phenomena such as the Purcell effect,[1] strong coupling,[2] and low-threshold lasing.[3]

It is expected that the combination of both III-N materials and photonic crystal membranes could lead to advanced optoelectronic devices in the UV-visible range operating at room temperature. Nevertheless, only few works have been reported on the fabrication of (III-N)-based photonic crystal membrane emitters. Indeed, nitride-based high-quality photonic crystal membranes are not easy to fabricate because the chemical inertness of III-N materials make their processing difficult. Moreover, photonic crystal structures optically active at short wavelengths require a very short lattice constant, typically between 100 and 200 nm and hole sizes between 50 and 150 nm. The first III-N photonic crystals were obtained with layers grown on sapphire substrates.[4,5] III-N photonic crystal surface emitting lasers at blue-violet wavelengths were demonstrated by electrical pumping of structures grown on GaN substrates[6] or under optical pumping for structures combining the slow modes of a two-dimensional photonic crystal coupled with a one-dimensional Bragg mirror.[7] Convex air-bridge AlN nanocavities processed on SiC substrate have been fabricated by photoelectrochemical etching leading to quality factors up to 2400 at 383 nm for a long $L7$ cavity.[8] Two-dimensional photonic crystal GaN suspended membranes have been reported on silicon substrate but without any optical characterization.[9] Moreover, there are no reports on AlN photonic crystal membranes containing emitters like quantum dots integrated on a silicon substrate. Integration on silicon is however of tremendous importance for the development of low cost optoelectronic devices in the blue-UV range.

In this letter, we report on the fabrication and the study of AlN photonic crystal membrane nanocavities with the embedded GaN quantum dots (QDs) for UV-visible emission at room temperature. To avoid problems encountered with the AlN etching, an original fabrication process of III-N photonic crystal membranes was developed. A nitride photonic crystal membrane is realized by performing a two-dimensional conformal nitride epitaxial growth by ammonia-based molecular beam epitaxy (NH$_3$-MBE) on a patterned silicon substrate followed by selective etching between silicon and III-N material. This innovative technique relies on the silicon technology processing and circumvents the difficulty associated with the etching of III-N materials.

The studied photonic crystal samples were fabricated by using four main processing steps. First, a silicon substrate is nanopatterned following a triangular lattice of air holes (Fig. 1(a)). A lattice period $a = 170$ nm is chosen in order to obtain a photonic band gap around 425 nm for a final hole radius after processing $r = 0.23a$ (~ 40 nm). A 90 nm-thick layer of ZEP-520A resist is spun directly on a (111) silicon substrate and is insolated with a 30 keV Raith e-beam lithography system. Patterns are then transferred to silicon by inductively coupled plasma etching in two steps. First, the pattern is initiated by an anisotropic etching. The holes are then etched using the Bosch process that consists in switching periodically between an SF$_6$ etching phase and a C$_4$F$_8$ sidewall passivation phase. This process is very selective and allows to use thin resist thickness, which is technologically
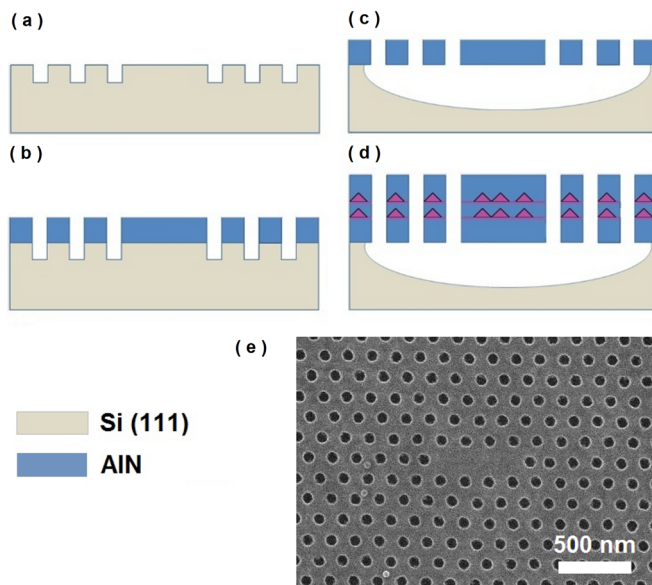
FIG. 1. (Color online) Schematic view of the fabrication steps. (a) Processing of photonic crystal in silicon (111) substrate by electronic lithography and inductively coupled plasma etching. (b) Conformal growth of 15 nm of AlN by NH_3-MBE on the nanopatterned substrate. (c) Underetching of the silicon substrate by HNA etching. (d) NH_3-MBE conformal growth of 85 nm of AlN with two GaN QDs planes. (e) Scanning electron microscope image of a modified L3 photonic crystal membrane nanocavity. The period and the hole radii of the AlN photonic crystal are 170 nm and 40 nm, respectively. The side holes of the cavity are moved to the edge by $d = 0.2a$ to increase resonance efficiency.

compatible with the small size of the desired nanopatterns. In a second step, a 15 nm-thick AlN layer is conformally grown on the patterned silicon substrate by NH_3-MBE (Fig. 1(b)).[10,11] We emphasize that the nanopatterning does not degrade the silicon surface and good quality epitaxial growth is achieved. The silicon is then underetched by a HF/nitric acid/acetic acid (HNA) solution in order to release the strain in the structure and to fabricate a membrane (Fig. 1(c)). An 85 nm-thick layer of AlN is then further conformally grown on the patterned substrate by NH_3-MBE, the total AlN thickness corresponding to a $\lambda/2n$ layer at 425 nm. Two planes of GaN quantum dots separated by a 10 nm AlN spacer are inserted into the middle of the AlN layer during the epitaxy (Fig. 1(d)). Controlled growth of very thin GaN QD epilayers on silicon substrates and their high emission efficiency at room temperature around 400 nm have previously been evidenced.[10,11] This fabrication process has been optimized taking into account that some parasitic material deposition occurs on the vertical silicon side walls. That could prevent a good underetching step. It explains why the epitaxial growth is interrupted after a first very short growth step (almost no side wall parasitic material deposition) and then the longer second growth step is carried out only after the underetching step. The underetching depth is around 750 nm, a thickness sufficiently large to ensure a decoupling of the optical mode from the substrate. Various types of nanocavities were fabricated, in particular L3 modified cavities. The L3 modified cavities are defined by three missing air holes with the edge air holes laterally shifted by a fraction of the lattice parameter ($d = 0.2a$).[12] Figure 1(e) shows a scanning electron microscope image of such a membrane cavity.

Microphotoluminescence (μ-PL) measurements were performed using a non-commercial microscope with a spot diameter of approximately 1.5 μm (power density 50 W cm^{-2}).[13] For quality factor measurements, the μ-PL signal was dispersed by a high-resolution spectrometer (3600 lines/ mm, 55 cm focal length) with a spectral resolution of ~ 0.16 meV. Spectroscopic measurements were performed at room-temperature with a 266 nm CW laser (Crylas/FQCW 266-50) and a spectrometer with a liquid nitrogen-cooled CCD. Figure 2 shows the room-temperature photoluminescence spectrum of a modified L3 cavity. Three resonant modes are evidenced around 2.910 eV, 2.975 eV, and 2.995 eV. Similar measurements were performed on a standard L3 cavity. Without edge holes displacement, the lowest energy mode is hardly observed and the higher-energy modes are spectrally shifted, in agreement with modeling (not shown). These resonances are thus not associated with the slow-modes of the photonic crystal but with the resonant modes of the cavity. A zoom of the spectrum of the fundamental mode with the highest quality factor is shown in the inset of Fig. 2. A quality factor of 1800 is achieved at 2.912 eV (425 nm). The small shift in the peak position between the two measurements can be likely explained by thermal effects occurring during the measurements, especially at high excitation power. Also, it was observed that the quality factor decreases as the pumping power is increased because of additional absorption losses due to free carriers photocreated in the membrane.[14]

For a better understanding of these results, the cavity was simulated using three-dimensional finite-difference in time domain calculations (3D-FDTD).[15,16] Dimensions used in the calculations were those obtained from the scanning electron microscope images. We used a refractive index of 2.15 for the AlN at 400 nm.[17] The 3D-FDTD spectrum is shown in Fig. 3. Three resonant modes are calculated for the modified L3 cavity at energies 2.847 eV, 2.932 eV, and 2.955 eV, along with a broader emission at 3.05 eV. Their quality factors are 4810, 485, and 1370, respectively, as compared to
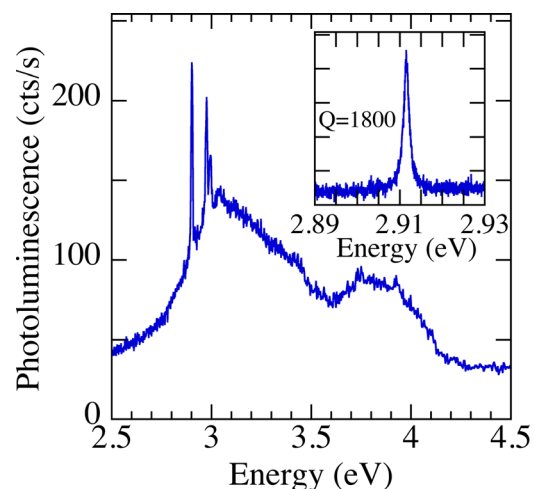

FIG. 2. (Color online) Experimental room temperature spectrum of a modified L3 nanocavity with a lateral shift $d = 0.2a$. The high-energy recombination feature, around 3.8 eV, is associated with lowest-height QD emission. The low-energy recombination component, around 3 eV, corresponds to large-height QD emission. Inset: spectrum with a high resolution grating (3600 lines/mm) of the lowest-energy mode. A Q factor of 1800 is obtained.
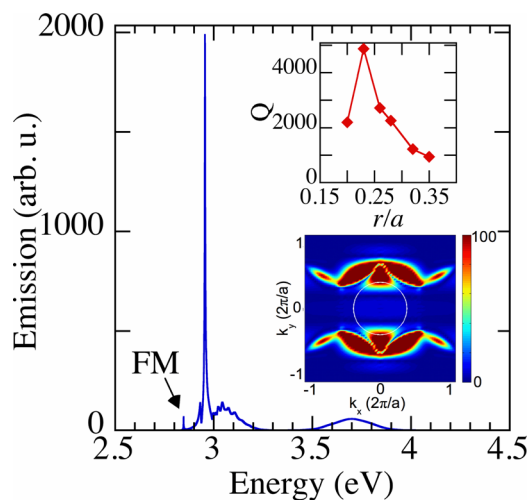
FIG. 3. (Color online) 3D-FDTD spectrum of the modified *L*3 nanocavity. The fundamental mode (FM) is indicated by an arrow. The top inset shows the evolution of the Q factor of the fundamental mode as a function of the hole radius. The bottom inset shows the two-dimensional Fourier-transform of the electric field distribution of the fundamental mode. The leaky region or light cone is highlighted.

1800, 270, and 270 experimentally. The spectrum is dominated by the mode at 2.955 eV, the two other modes having in the modeling a significantly smaller amplitude. A satisfying agreement is obtained between experiments and modeling for the energy position of the modes and their energy spacing. Since Fig. 3 represents the spectrum of the simulated field on the top of the membrane, the amplitude of each component is different from the experimental one that is indeed a far field spectrum spatially filtered by the microscope objective.[18] Experimentally, the quality factor of the fundamental mode is only 2.5 times smaller than the calculated one. We attribute the discrepancy to the inhomogeneities of the air holes, to the hole roughness, and to the reduced symmetry of the holes, which are not perfect circles. We emphasize that the calculated quality factors for AlN membrane cavities are significantly smaller than those that can be obtained with silicon photonic crystal membrane-type *L*3 cavities (typically 100 000 for optimized structures).[14,19] Indeed, the smaller value of the refractive index of AlN as compared to silicon (2.15 vs. 3.45) decreases significantly the photonic band gap width. Moreover, the associated normalized frequency is around 0.4 instead of 0.25, and the Fourier components inside the air escape cone are significantly larger as compared to silicon membranes, leading to a decreased quality factor (see inset of Fig. 3). The quality factor of the fundamental mode is very sensitive to the cavity design and to the air hole radius (second inset of Fig. 3). A sharp maximum is obtained for a radius $r = 0.23a$ corresponding to the investigated structure. Experimentally, we have measured a quality factor of 1170 at 417 nm for a r/a value of 0.25, corresponding to a 35% decrease from the maximum, consistent with the modeling.

One possible prospect for such small volume/high Q cavities would be to obtain a UV nanolaser. Taking into account the Purcell effect in the framework of rate equations for the cavity/QD system, the lasing conditions reads $\xi = \frac{N_t \beta}{2 \tau_e \gamma_c} > 0.25$, where N_t is the number of QDs that spatially and spectrally match the mode, β is the spontaneous emission coupling factor to the cavity mode, τ_e is the average spontaneous emission rate of the QDs in the mode, and γ_c is the photon escape rate out of the cavity.[20] For this lasing evaluation, the homogeneous linewidth is not a critical parameter: as the homogeneous linewidth increases, the decrease of the Purcell effect is compensated by the increased number of dots resonant with the optical mode. It is however now well known that, in the case of very small QD-based lasers showing a large Purcell effect, the mere rate equations do not take into account all the processes leading to gain and that lasing can actually be achieved with ξ values smaller than predicted as shown in Ref. 21 for which lasing is achieved with $\xi = 6 \times 10^{-2}$. In the present case, N_t is around 2, the Purcell factor is about 200, leading to $\beta \sim 1$. The natural spontaneous emission rate for such large GaN QDs undergoing a strong quantum confined Stark effect is about 200 ns for an emission at 3 eV,[22] yielding an average spontaneous emission rate τ_e due to the Purcell effect of 4 ns, taking into account an average decrease of the Purcell factor by 4 due to spectral and spatial mismatch between the dots and the mode. This gives $\xi = 1 \times 10^{-4}$. One sees that the present cavity is far from reaching lasing conditions. However, the new process presented here should be transposable to much shorter wavelengths (around 300 nm emission) for which the GaN/AlN QD natural lifetime is much shorter, around 0.5 ns. It is reasonable to expect to gain a factor of two on the QD density by increasing the number of QD planes and to increase further the quality factor to reach 4000. This would give a ξ around 0.1, which gives reasonable hope to reach UV (around 300 nm) lasing in such a nanolaser.

[1] A. Badolato *et al.*, Science **308**, 1158 (2005).
[2] T. Yoshie *et al.*, Nature (London) **432**, 200 (2004).
[3] M. Loncar *et al.*, Appl. Phys. Lett. **81**, 2680 (2002).
[4] T. N. Oder *et al.*, Appl. Phys. Lett. **83**, 1231 (2003).
[5] Y.-S. Choi *et al.*, Appl. Phys. Lett. **87**, 243101 (2005).
[6] H. Matsubara *et al.*, Science **319**, 445 (2008).
[7] T.-C. Lu *et al.*, Appl. Phys. Lett. **93**, 111111 (2008).
[8] M. Arita *et al.*, Appl. Phys. Lett. **91**, 051106 (2007).
[9] A. Rosenberg *et al.*, J. Vac. Sci. Technol. B **25**, 721 (2007).
[10] S. Sergent *et al.*, Appl. Phys. Express **2**, 051003 (2009).
[11] S. Sergent *et al.*, J. Appl. Phys. **109**, 053514 (2011).
[12] Y. Akahane *et al.*, Nature (London) **425**, 944 (2003).
[13] M. Mexis *et al.*, Opt. Lett. **36**, 2203 (2011).
[14] M. El Kurdi *et al.*, Opt. Express **16**, 8780 (2008).
[15] X. Checoury *et al.*, Appl. Phys. Lett. **86**, 151111 (2005).
[16] Z. Han *et al.*, Opt. Comm. **283**, 4387 (2010).
[17] N. Antoine-Vincent *et al.*, J. Appl. Phys. **93**, 5222 (2003).
[18] J. Vuckovic *et al.*, IEEE J. Quantum Electron. **38**, 850 (2002).
[19] Y. Akahane *et al.*, Opt. Express **13**, 1202 (2005).
[20] J.-M. Gérard in *Photonic Crystals: Towards Nanoscale Photonic Devices*, edited by J.-M. Lourtioz, H. Benisty, V. Berger, and J.-M. Gérard (Springer, Berlin, 2008).
[21] S. Strauf *et al.*, Phys. Rev. Lett **96**, 127404 (2006).
[22] T. Bretagnon *et al.*, Phys. Rev. B **73**, 113304 (2006).